ORGANOMETALLICS

pubs.acs.org/Organometallics
Article

Phosphinoyl-Substituted Ketenyl Anions: Synthesis and Substituent Effects on the Structural Properties

Mike Jörges, Sunita Mondal,[†] Manoj Kumar,[†] Prakash Duari,[†] Felix Krischer, Julian Löffler, and Viktoria H. Gessner*

Cite This: *Organometallics* 2024, 43, 585−593
Read Online

ABSTRACT: Ketenyl anions are versatile intermediates in synthetic chemistry and have recently become accessible as isolable reagents from metalated ylides by exchange of the phosphine with CO. Herein, we report on a systematic study of substituent effects on the structure and bonding situation in ketenyl anions. A series of phosphinoyl-substituted ketenyl anions {$[R_2P(X)CCO]^-$ with X = O, NTol, S, Se} were prepared by carbonylation of the corresponding yldiides and isolated as their corresponding potassium salts. NMR and IR spectroscopic analyses together with computational studies demonstrate that the more electron-withdrawing oxo- and iminophosphinoyl substituents increase the s-character in the bond to the ketene moiety and hence the ynolate character of the anion. This trend is particularly seen in solution, whereas the solid-state properties are influenced by packing effects affecting the bonding situation.

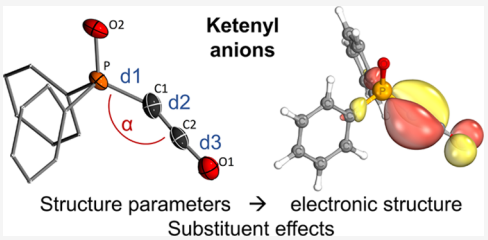

INTRODUCTION

Ketenes, $R^1R^2C{=}C{=}O$, have first been synthesized and isolated more than 100 years ago and since then become indispensable intermediates and reagents in synthetic chemistry.[1,2] This is primarily due to their unique reactivity, which allows for a myriad of reactions to a variety of different carbonyl containing compounds. Due to their high reactivity, ketenes are often synthesized in situ and directly converted to the desired product.[2−6] Until now, several synthetic routes to ketenes have been developed, which however are often limited with respect to their substrate scope, yield, and practical feasibility.

Ketenyl anions, $[RC{=}C{=}O]^-$, represent a convenient entry into ketene chemistry. They have been known as reactive intermediates since several years and reported to be viable precursors to ketenes and other carbonyl containing compounds.[7] The first synthesis of a ketene anion was reported by Schöllkopf and Hoppe by lithiation of 3,4-diphenylisoxazole followed by their fragmentation with concomitant elimination of benzonitrile (Figure 1A).[8] Later, various other methods to anionic ketene intermediates were reported among their synthesis by carbonylation of lithiated diazomethanes or metalation of silylketenes or dibromoenolates.[9−19] Albeit various further transformations with different electrophiles were reported, no isolation of a stable ketenyl anion was achieved at that time. In 2021, the group of Stephan reported the intermediate formation of the anionic ketene, $[Ph_2P(S)C{=}C{=}O]^-Li^+$ from the reaction of a dilithiomethandiide with CO and N_2O. Although the isolation of the ketenyl anion was not possible, it could be characterized by multinuclear magnetic resonance (NMR) spectroscopy.[20]

The first isolation and structure elucidation were recently accomplished by our group based on a new synthetic route starting from metalated ylides **IIa** and **IIb** (Figure 1B).[21] Phosphine displacement at the ylidic carbon atom in **II** with CO as an inexpensive sustainable building block enabled the high-yielding formation of the corresponding ketenyl anions **I**. The selectivity of the phosphine-CO replacement was found to strongly depend on the reaction conditions, in particular the solvent, additives for coordination of the metal cation, as well as the nature of the alkali metal and the phosphine substituent.[22] Depending on the chosen conditions, either formation of the ketenyl anion **I** or phosphoranylideneketene **III** via metal salt elimination was observed.[23] Shortly after our publication, the Liu group also reported on the isolation and structure elucidation of a ketenyl anion formed by carbonylation of a phosphinoyl-substituted metalated diazomethane, which they furthermore could oxidize to the corresponding selenide.[24] Structure elucidation in combination with computational studies of the ketenyl anions revealed an intermediate bonding situation between a ketene **I** and an ynolate form **I'**. Thus, shorter C−C bond lengths than typical double bonds but still shortened C−O distances relative to C−O single bonds were observed in the crystal structures. Nonetheless, the ketenyl anions underwent selective reactions at the carbon atom rather

Received: December 22, 2023
Revised: January 26, 2024
Accepted: January 30, 2024
Published: February 15, 2024

https://doi.org/10.1021/acs.organomet.3c00530
Organometallics 2024, 43, 585−593

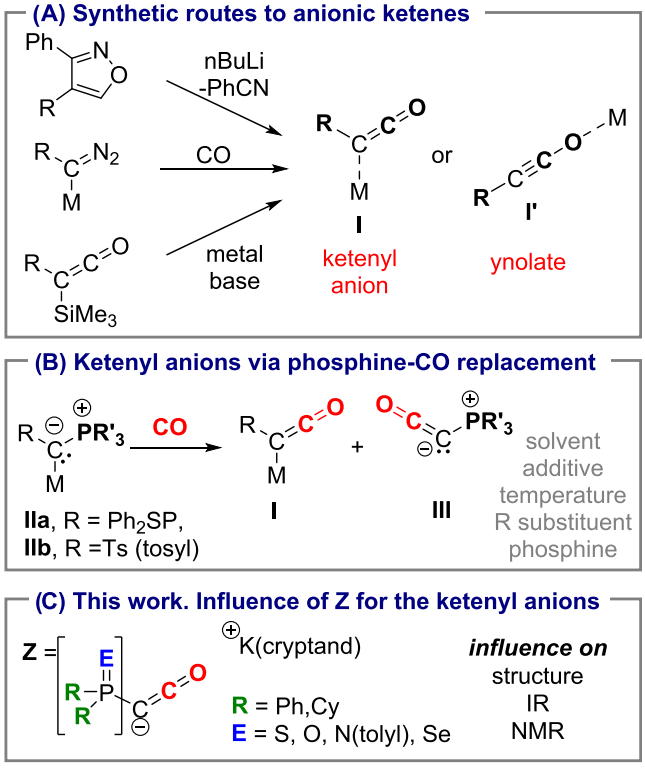

Figure 1. (A) Selected synthetic routes to ketenyl anions, (B) ligand exchange in metalated ylides, and (C) structures of ketenyl anions examined in this work.

than at the oxygen end, highlighting the importance of the ketene structure **I**.

Despite the mild access to ketenyl anions via ligand exchange in metalated ylides, this method is limited by the availability of yldiide precursors. Till now, only four ketenyl anions have been structurally characterized, all featuring different coordination modes of the metal. Since the coordination of the metal may itself influence the structure formation and hence important parameters such as bond angles and distances, no direct comparison of the reported structures is possible. This leaves the question of how the Z group affects the structure of these compounds unanswered. In order to elucidate the impact of different substituents on the structure of ketenyl anions, we targeted the synthesis of a series of ketenyl anions with different phosphinoyl Z groups to examine the impact of the different anion-stabilizing abilities of the Z moiety on the ligand exchange reaction, the bonding situation and structure of the anions, and their stability.

RESULTS AND DISCUSSION

Synthesis of the Metalated Ylides and Ketenyl Anions.

We started our investigations with the synthesis of a series of metalated ylides with phosphinoyl moieties varying in the P = E linkage (E = N(*p*-Tol), O, S, Se) as well as the organic substituents R (R = Ph, Cy). Both, the E and R group should influence the anion-stabilizing ability of the phosphinoyl group due to their different capacities to delocalize electron density via negative hyperconjugation effects. The corresponding ylides **1a** and **1b** were initially prepared via salt elimination reaction from commercially available compounds and could be isolated as yellow solids in high yields (see the SI for details; Scheme 1). The oxidation of ylide **1** to **2-S** and **2-Se** was subsequently

Scheme 1. Preparation of the Ylide Precursors 2-E

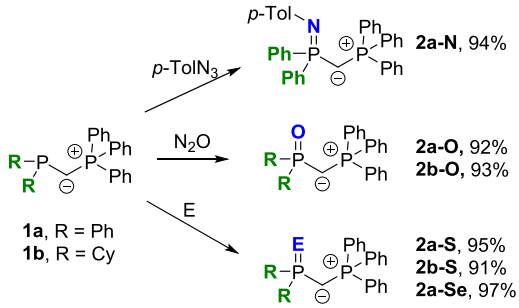

accomplished with one equivalent of elemental sulfur or selenium in THF, whereas **2-N** and **2-O** were obtained from the reaction of **1** with *para*-tolyl azide and N_2O, respectively. In all cases, the ylides were isolated as colorless solids in high yields of over 90%.

Subsequently, the oxidized ylides were converted into the metalated ylides **3** using strong metal base (Scheme 2). In most

Scheme 2. Preparation of the Ketenyl Anions 4[a]

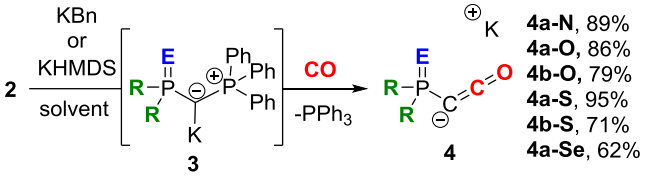

[a]Solvent = toluene (for E = N,O,S) or a toluene/THF mixture (for E = Se).

cases, benzyl potassium was employed as a base and toluene as a solvent. Other combinations of bases and solvents turned out to be less effective, either due to low conversion or byproduct formation. Sole exception was the reaction of **2-Se**, which led to the reduction of the phosphine selenide under these conditions. This side reaction could be prevented by using KHMDS (potassium hexamethylsilazide) as a base in a THF solution. It must be noted that we deliberately selected potassium bases for the formation of yldiides **3** since we only targeted ketenyl anions with potassium as the cation to allow a discussion of the bonding situation independent of influences of different metals. In previous studies, the potassium yldiides have shown higher selectivities in the subsequent carbonylation reaction in comparison to their lithium or sodium analogues and were thus selected for these studies.[23] In each case, the successful formation of the metalated ylides **3** was proven by in situ NMR spectroscopy, but the compounds were not isolated due to their high reactivity and their effective in situ transformations. In the case of the iminophosphorane **3a-N** few single crystals suitable for X-ray diffraction (XRD) analysis could be obtained from a diethyl ether solution, which unambiguously confirmed the successful α-metalation.

In the crystal structure of **3a-N** (Figure 2), the metalated ylide forms a dimeric structure, with the potassium cations being coordinated by the nitrogen of the iminophosphinoyl moiety, the ylidic carbon atom, and an additional diethyl ether molecule. The P−C distances of 1.656(2) and 1.627(2) Å are significantly shorter than in the ylide structure **2a-N** (1.736(2) and 1.695(2) Å), which is caused by increased electrostatic interactions in the P−C−P linkage. At the same time, the bonds between the phosphorus atoms and their substituents (P−N and P−C_{Ph})

https://doi.org/10.1021/acs.organomet.3c00530
Organometallics 2024, 43, 585−593

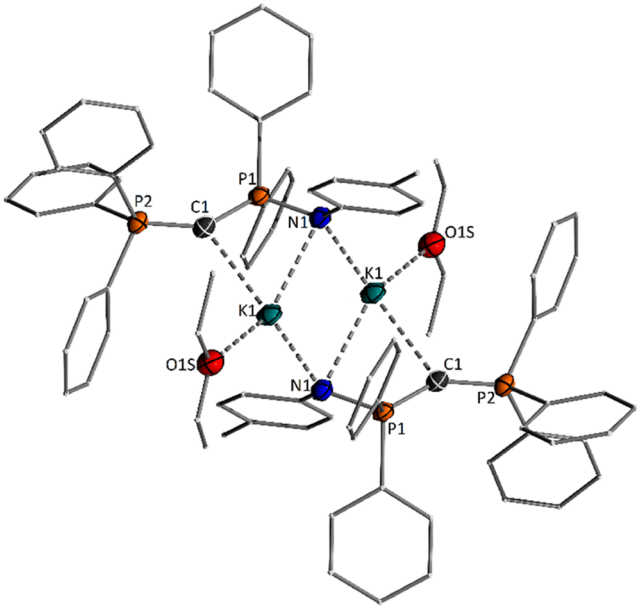

Figure 2. Structure of the metalated ylide **3a-N** in the solid state. The structure of **2a-N** is depicted in the Supporting Information. Important bond lengths (Å) and angles (°) of **3a-N** and **2a-N**. **2a-N**: C1−P1 1.736(2), C1−P2 1.695(2), P1−N1 1.585(2), P−C−P 126.76(11), **3a-N**: C1−P1 1.656(2), C1−P2 1.627(2), P1−N1 1.633(2), P−C−P 143.87(14). The predominant ionic interactions with the potassium cation are shown in dashed lines.

elongate because of negative hyperconjugation effects. Both effects are typical for metalated ylides and contribute to the stability of these compounds.[25−28] They are in general on little affected by the aggregation of the compounds since the predominantly ionic interactions to the alkali metal cations have only a small influence on the charge on the central carbon atom.[25−28]

In general, the metalated ylides **3** are characterized by a significant high-field shift of the $^{31}P\{^{1}H\}$ NMR signal compared to the ylide precursors and therefore easy to identify by NMR spectroscopy (Table 1). Furthermore, the metalation is accompanied by a significant increase of the $^{2}J_{P,P}$ coupling constants, e.g., from 19.4 for the iminophosphinoyl substituted ylide **2a-N** to 88.1 Hz in its metalated congener. These trends have been reported earlier for other metalated ylides and are well in line with the increasing charge at the ylidic carbon atom and the resulting shortening of the P−C bond.[25−30]

After having confirmed the selective formation of the metalated ylides **3**, they were directly reacted in toluene with one atm of CO at room temperature. Stirring overnight resulted in the precipitation of potassium complexes of the ketenyl anions from the reaction mixture, which could thus be obtained as colorless solids by filtration in good to excellent yields (Scheme 2). In none of the cases, competing elimination of the metal salt $R_2P(E)K$ with concomitant formation of the phosphoranylideneketene Ph_3PCCO (c.f. **III** in Figure 1B) was observed by $^{31}P\{^{1}H\}$ NMR spectroscopy.

Comparative NMR spectroscopic studies of ketenyl anions **4** were conducted in THF solution (Table 2). Unexpectedly, the solubility of the cyclohexyl-substituted anion **4b-O** was significantly lower in this solvent than that of its phenyl analogue **4a-O**. Therefore, the more polar solvent DMSO was used for spectroscopic analyses of **4b-O**. Comparison of the obtained NMR data of the ketenyl anions **4**, ylides **2**, and metalated ylides **3** shows that there is no clear trend visible in the ^{31}P chemical shifts with varying E. However, the shifts follow a systematic pattern. Within the series of group 16 compounds, the selenides always show the most upfield-shifted signal for the phosphinoyl group, whereas the sulfur compounds consistently feature the most deshielded signals. The iminophosphoranes (E = N(tolyl))—despite nitrogen having an electronegativity of 3.0, i.e., between oxygen and sulfur—showed the most high-field-shifted ^{31}P signals, clearly demonstrating that there is no correlation of the NMR chemical shift and the electronegativity of E. The influence of the substituents R is much clearer and as expected. Replacing the phenyl groups with cyclohexyl groups results in a shift into the low-field region, while the carbon signals become upfield-shifted. This correlates well with the stronger electron-donating ability of the cyclohexyl groups. The ^{13}C NMR shift of the C1 carbon atom of the CCO moiety also experiences a slight high-field shift in the order of O > S = Se, thus suggesting an increasing carbanion character in this series of compounds.

Table 2. NMR Spectroscopic Data of the Ketenyl Anions in THF-d_8 ([4b-O]K in DMSO-d_6)[a,b]

	4a-N	4a-O	4b-O	4a-S	4b-S	4a-Se
δ(P)	−6.9	13.2	31.5	22.5	43.2	6.2
δ(C1)	−0.66	3.11	0.17	2.42	−2.39	2.51
$^{1}J_{P,C}$	184	210	183	175	152	164
δ(C2)	141.1	140.8	135.6	142.7	139.9	143.9
$^{2}J_{P,C}$	41.3	47.5	39.8	40.7	35.2	39.0

[a]Values correspond to the potassium compounds. [b]NMR shifts are given in ppm and coupling constants in Hz.

In contrast to the NMR chemical shifts, the coupling constants in the ketenyl anions follow systematic trends according to the expected electronic properties. Thus, the $^{1}J_{P,C}$ coupling constant decreases from 210 to 164 Hz in the order O > N > S > Se (for R = Ph), i.e., with decreasing electronegativity of E. This corroborates well with the decreasing *p*-character in the P−E bond of the more electropositive elements (Bent's rule),[31] which ultimately leads to an decreased s-character in all other bonds and hence in lower coupling constants. In the same vein, changing from R = Ph to R = Cy also results in a decreasing $^{1}J_{P,C}$ coupling constant. The $^{2}J_{P,C}$ coupling constants in the ketenyl

Table 1. NMR Spectroscopic Data of the Ylides and the Metalated Yldiides in C_6D_6[a]

	2a-N	2a-O	2b-O	2a-S	2b-S	2a-Se	3a-N	3a-O	3b-O	3a-S	3b-S	3a-Se
δ(PE)	3.9	26.3	49.0	35.9	53.3	21.9	−15.4	23.0	44.2	20.3	44.0	−1.34
$^{2}J_{P,P}$	19.4	18.7	12.7	28.4	19.6	31.5	88.1	97.8	102.9	56.2	56.6	44.1
δ(C1)	7.4	11.8	4.4	11.1	5.4	9.2						
$^{1}J_{P,C}$	126.7, 113.3	120.3, 106.5	113.6, 104.9	122.0, 106.9	126.1, 90.7	122.9, 98.8						

[a]NMR shifts are given in ppm and the coupling constants in Hz.

https://doi.org/10.1021/acs.organomet.3c00530
Organometallics 2024, 43, 585−593

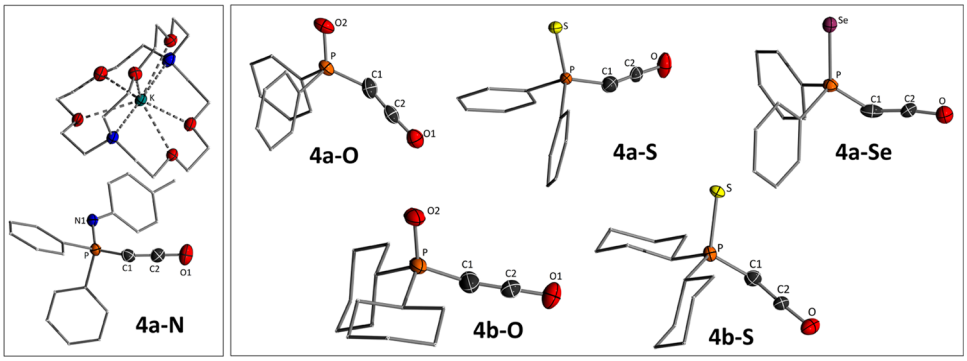

Figure 3. Molecular structures of potassium ketenyl anions **4** with a cryptand as the coordinating ligand in the solid state. The [K@cryptand]$^+$ cation is only shown for the iminophsphorane **4a-N.** Thermal ellipsoids are shown at the 50% probability level. Important bond lengths and angles are given in Table 3, and crystallographic details are given in the Supporting Information.

Table 3. Important Bond Lengths and Angles of the [K@cryptand]$^+$ Salts of Ketenyl Anions 4

	4a-N	4a-O	4b-O	4a-S[a]	4b-S[a]	4a-Se[a]
P−E [Å]	1.597(2)	1.496(2)	1.498(2)	1.991(1)	2.043(3) 2.023(5)	2.145(5)
P−C [Å]	1.689(2)	1.686(2)	1.694(2)	1.670(7)	1.662(15) 1.613(15)	1.699(12)
C−C [Å]	1.250(3)	1.240(2)	1.219(3)	1.244(5)	1.263(12) 1.245(13)	1.220(11)
C−O [Å]	1.201(3)	1.212(2)	1.202(2)	1.207(4)	1.215(8) 1.207(11)	1.201(4)
P−C−C [°]	143.6(2)	148.9(2)	160.1(2)	151.6(8)	142.6(17) 149.2(18)	159.6(12)
C−C−O [°]	174.8(2)	175.1(2)	176.0(2)	176.2(6)	173.2(12) 173.9(19)	175.8(9)

[a]The crystal structures of **4b-S**, **4a-S**, and **4a-Se** contain a disorder of the ketenyl and phosphinoyl moiety (see the SI for further details). For **4b-S**, both parts of the disorder showed equal occupation. Therefore, the values of both components are discussed. For **4a-S** and **4a-Se**, the minor component showed an occupation of only 17 and 15%, respectively. Hence, only the main structures are discussed.

anions **4** also slightly decrease in the same order. Overall, the coupling constants and NMR shifts suggest that for R = Ph and E = O or NTol, the P−C bond has the highest s-character, which should lead to a slight stabilization and preference of the ynolate resonance structure **I'**.

Crystal Structure Analyses of the Ketenyl Anions. Next, we aimed to gain further insights into the bonding situation by crystallographic studies. Such structural insights are particularly important because only a few ketenyl anions have been structurally characterized to date, and all have been determined under different conditions (solvent, additive), limiting meaningful comparisons. Previous studies have shown that the metal cation can bind to the oxygen, the ketenyl carbon atom, or both sites depending on the nature of the metal and additional coligands. To guarantee the comparability of the structures, we decided to initially focus our investigations on solvent/ligand-separated ion pairs of the potassium salts. In this way, we expected a possible discussion of the structural parameters without disturbing metal interactions.

Addition of crown ethers to the ketenyl anions allowed us to crystallize the ketenyl anions as monomeric complexes.[21] However, the cation was found to still coordinate to the ketenyl anion, which prompted us to employ [2,2,2]cryptand to fully encapsulate the cation to yield the "naked" ketenyl anions. Indeed, this approach enabled us to determine the crystal structures of all five ketenyl anions as ligand-separated ion pairs (Figure 3). Important angles and distances of all structures are summarized in Table 3. Comparison of these parameters shows that the P−E bonds elongate as expected with decreasing electronegativity and increasing atomic radius of E, i.e., in the order O < N < S < Se. Within this order, the P−C distances seem to slightly decrease when comparing the oxides and sulfides with each other. This might be attributed to the weaker ability of the heavier elements to stabilize the positive charge at the phosphorus atom, which therefore more strongly interacts with negatively charged C1 atom. This is confirmed by density functional theory (DFT) studies showing a decreasing remaining negative charge at the carbon atom C1 when descending the group (see below).

Nevertheless the changes in the P−C bond lengths are less uniform compared to the P−E distances. The same applies to the C1−C2 and C2−O bonds, which do not follow any obvious trends. Both bonds undergo a change of approximately 0.02 Å, which is too small to derive meaningful information. In addition, most structures feature disordered ketenyl moieties (not shown in Figure 3), some of which have significantly different bond distances and angles in the P-CCO unit (see the Supporting Information for details, Figure 4), which may override underlying trends. In these disorders, the CCO and group 16 element E change their positions, resulting in additional electron density between the C1 and C2 carbon atoms, making it difficult to exactly locate their position. This is particularly true for the selenium compound, in which a minor disorder of the P−Se linkage already significantly impacts the structure refinement.

https://doi.org/10.1021/acs.organomet.3c00530
Organometallics 2024, 43, 585−593

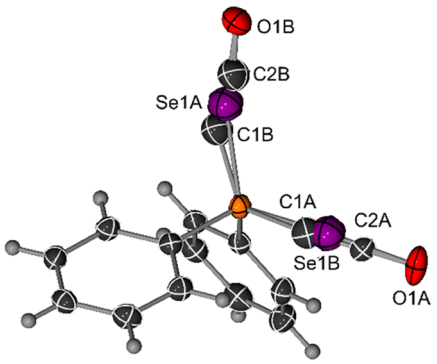

Figure 4. Display of the molecular structure of the selenium ketenyl anion **4a-Se** showing the disorder of the P-CCO and P−Se linkage. Thermal ellipsoids are shown at the 50% probability level.

These disorders were repeatedly found in the crystals of the sulfides and selenides even when crystallized under different conditions.

In order to probe whether coordination of the metal cation influences the structure parameters of the anions, crystallization of the cryptand/crown ether free complexes was attempted. Single crystals suitable for XRD analysis could be obtained for **4a-N** and **4b-S** from THF solutions (Figure 5). The structure of **4a-S** without cryptand has previously been reported.[21] The complexes crystallize as coordination polymers in which the potassium cation binds to both the C1 carbon atom and the oxygen center of the ketenyl moiety. In each case, the coordination sphere of the metal is completed by the additional coordination of THF and the nitrogen or sulfur atom of the phosphinoyl moiety. **4a-N** features one molecule of the ketenyl anion in the asymmetric unit, which forms a centrosymmetric dimeric subunit of polymer $[(\mathbf{4a\text{-}N})K(THF)]_\infty$ (Figure 5b). The central structural motif of this subunit is formed by a $K_2O_{2(THF)}$ four-membered ring, with the potassium ions being additionally coordinated by the tolyl group of the iminophosphinoyl moiety. In contrast, **4b-S** features two molecules in the asymmetric unit (Figure 3b) with differently coordinated potassium ions. K1 is bound by the oxygen and sulfur atoms of the ketenyl as well as one THF molecule, whereas K2 is placed in the pocket of the two ketenyl molecules, forming contacts to all atoms of the C−C−O moiety.

Comparison of the structure parameters of the naked ketenyl anions with the corresponding contact ion pairs revealed no systematic changes. This is most likely due to the coordination of the metal ion to all partially negatively charged sites (E, C1, and O) in the anions, thus resulting in no significant changes at a specific position in the molecule. However, it is noteworthy, that the P−C−C angle of 166.4(2)° in $[(\mathbf{4a\text{-}N})K(THF)]_\infty$ significantly differs from the angle in the free anion (143.6(2)°), thus confirming the high flexibility of this angle as was previously reported for the tosyl system **Ib**.[23] This change does not significantly affect the other bonding parameters.

IR Spectroscopic and Computational Studies. A further characteristic feature of ketenyl anions is the vibration of the ketene unit, which falls between those of ketenes and alkynyl ethers, with the latter being blue-shifted.[32] To determine the influence of the E substituents on the ketene vibrations, IR measurements of anions **4a-E** in the solid state with and without [2,2,2]cryptand were performed (Table 4). To also exclude solid-state effects on the vibration, we furthermore determined the stretching frequencies in THF solution.

The comparison of the IR data demonstrates that again, no clear trend with varying E is discernible from the solid-state data, independent of the presence or absence of the cryptand ligand. Again, we explain this observation with the flexible P−C−C angle, which can easily be influenced by packing effects, and the cation−anion interactions, which depending on the exact solid-state structure affect the bonding situation. This contrasts the spectra in THF solution, which show a trend toward smaller wavenumbers for the electropositive elements E, suggesting an

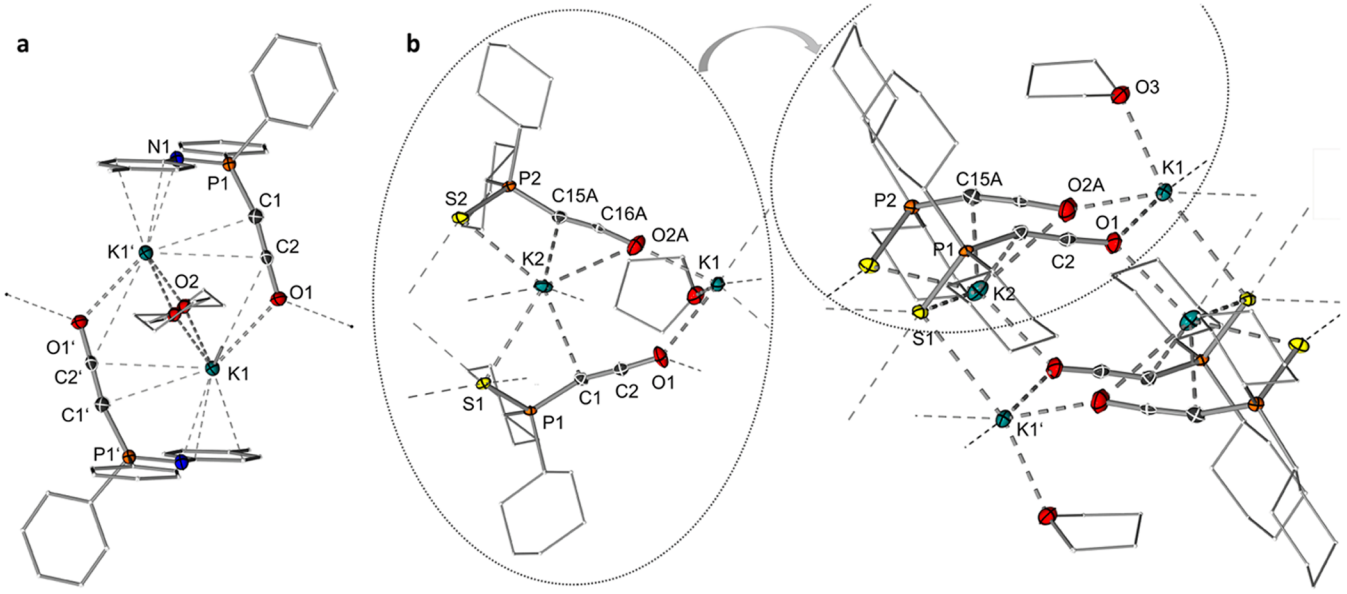

Figure 5. Molecular structures of (a) $[(\mathbf{4a\text{-}N})K(THF)]_\infty$ and (b) $[(\mathbf{4b\text{-}S})_2K_2(THF)]_\infty$ in the solid state. Crystallographic details are given in the Supporting Information. The asymmetric unit of $[(\mathbf{4b\text{-}S})_2K_2(THF)]_\infty$ contains two molecules of the potassium ketenyl and one molecule of THF. Since one of these ketenyl anions is highly disordered, only the parameters of the other molecule are given here. Selected bond lengths (Å) and angles [°]: $[(\mathbf{4a\text{-}N})K(THF)]_\infty$: C1−C2 1.222(2), C2−O1 1.225(2), P−C1 1.702(2), P−N1.592(2), P−C1−C2 166.4(2), C1−C2−O1 178.4(2), $[(\mathbf{4b\text{-}S})_2K_2(THF)]_\infty$: C1−C2 1.235(4), C2−O1 1.217(3), P−C1 1.704(3), P−S 2.007(1), P−C1−C2 150.9(2), and C1−C2−O1 175.5(3).

https://doi.org/10.1021/acs.organomet.3c00530
Organometallics 2024, 43, 585−593

Table 4. Stretching Frequencies of the Ketenyl Moiety in the Potassium Complexes of Ketenyl Anions 4 with and without Cryptand[a]

	solid state		THF solution	
	ligand-free	+cryptand	ligand-free	+cryptand
4a-N	2083.87	2098.95	2093.23	2094.84
4a-O	2093.92	2091.77	2092.03	2096.15
4a-S	2081.71	2080.28	2085.14	2086.61
4a-Se	2092.49	2089.61	2083.13	2082.90

[a]Vibrations are given in cm^{-1}.

increased preference of the ketenyl structure for these compounds. This is in line with our interpretation of the NMR parameters (decreasing coupling constant and high-field shift of C1 in the same order of compounds (see above)). This clearly demonstrates that conclusions drawn from spectroscopic properties of ketenyl anions in the solid state may be difficult to interpret due to the flexibility of the structure (disorder, angle at C1) and metal anion contacts, which affect the electronic properties of the compound and thus may override trends expected for the undisturbed structures.

To further support these interpretations, we conducted computational studies on the free anions **4a-E** in the gas-phase on the PBE0/def2-TZVPD level[33] of theory (see the Supporting Information for details). Intrinsic bond orbital (IBO) analysis[34] yielded localized orbitals reminiscent of an ynolate structure for all anions (Figure 6). However, the intrinsic atomic orbital

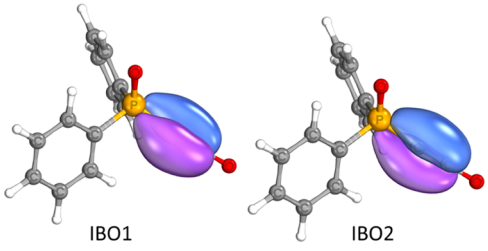

Figure 6. Representation of the intrinsic bond orbitals (IBO)[36] with the highest energies for **4a-O**.

(IAO) charges and Wiberg bond indices showed clear trends (Table 5), which confirm the experimental observations made by NMR and IR spectroscopy. As such, the charge at the phosphorus atom decreases with decreasing electronegativity of E, i.e., in the order O > *N* > S > Se. In the same way, the negative charge at C1 decreases, and the P−C bond indices increase, as was also indicated in the crystal structures of the compounds. The variation of the P = E moiety also systematically influences the ketenyl moiety. As such, the Wiberg bond index (WBI) of the C1−C2 bond decreases from oxygen to sulfur and selenium, while the WBI for the C−O bond increases in the same order. This supports our conclusion that the phosphinoyl (P = O) system exhibits the most pronounced ynolate character.

Table 5. Calculated Intrinsic Atomic Orbital (IAO) Charges and Bond Indices for the Phenyl-Substituted Ketenyl Anions 4 (B3PW91/def2-TZVPD)

	4a-O	**4a-S**	**4a-Se**	**4a-N**
		IAO charges		
q(P)	1.5670	1.1858	1.1190	1.4354
q(E)	−0.9984	−0.7360	−0.7067	−0.80989
q(C1)	−0.8238	−0.8134	−0.8064	−0.84309
q(C2)	0.3279	0.3473	0.3505	0.35451
Q(O)	−0.5007	−0.4746	−0.4692	−0.46756
		Wiberg bond indices		
P−E	1.1592	1.1691	1.1107	1.1004
P−C	1.0342	1.0681	1.0867	1.0509
C−C	2.1294	2.0820	2.0723	2.0666
C−O	1.7042	1.7413	1.7478	1.7519

CONCLUSIONS

In summary, we have prepared a series of phosphinoyl-substituted ketenyl anions by carbonylation of the corresponding metalated ylides with concomitant elimination of triphenylphosphine. These ligand exchange reactions proceeded in a highly selective manner and allowed the isolation of anions as potassium salts in high yields. Using [2,2,2]cryptand, all anions were crystallized as ligand-separated ion pairs, while the ligand-free salts of the sulfide and iminophosphinoyl systems formed coordination polymers. Unfortunately, the structural data obtained from the solid-state structures showed no obvious trends in the bonding situation with variation of the substitution pattern, presumably due to overriding effects from disorders or crystal packing. In contrast, the solution properties followed small but systematic trends, showing that the more electron-withdrawing substituents result in a slight preference of the ynolate structure in comparison with their more electropositive analogues. This can be seen from more low-field-shifted signals for the C1 carbon atom in the ^{13}C NMR spectrum, higher $^{1}J_{P,C}$ coupling constants, and higher stretching frequencies. These trends are supported by DFT studies, thus confirming the tunability of the properties of the ketenyl anions by the substitution pattern. Future experimental studies will explore how these differences can be used in synthetic applications.

EXPERIMENTAL SECTION

All experiments (if not stated otherwise) were carried out under a dry, oxygen-free argon atmosphere by using standard Schlenk techniques. Argon (99.999%) was purchased from Air Liquide. Solvents and chemicals: Involved solvents were dried using a MBraun SPS 7 (THF, toluene, diethyl ether, *n*-hexane, *n*-pentane, acetonitrile) or dried in accordance with standard procedures and stored under an argon atmosphere over 3 or 4 Å molecular sieves. Reagents were purchased from Sigma-Aldrich, ABCR, Acros Organics or TCI Chemicals and used without further purification if not stated otherwise. BnK,[35] **1a**, **2a-S**, **3a-S**, and **4a-S** were synthesized following literature procedures.[21] ^{1}H, $^{13}C\{^{1}H\}$, and $^{31}P\{^{1}H\}$ NMR spectra were recorded on an Avance III 400 spectrometer from Bruker at 25 °C. Chemical shifts are given in ppm regarding the δ scale and are referenced to the residual protons of the deuterated solvent. All spin−spin coupling constants are given in Hz. Multiplicities are indicated with the following abbreviations: s = singlet, d = doublet, t = triplet, q = quartet, dt = doublet of triplets, etc. The assignment of signals was supported by HSQC, HMBC, APT, and COSY experiments.

Procedures for the synthesis of the starting materials are given in the Supporting Information.

Synthesis of 4a-N. 1.0 g (1.8 mmol) of compound **2a-N** and 276 mg (2.1 mmol) of benzyl potassium were dissolved in 10 mL of toluene and stirred for 30 min at room temperature. After filtration, the atmosphere in the flask was changed from argon to CO, and the reaction mixture was stirred for 24 h. The solvent was removed under reduced pressure, and the solid was washed with toluene and pentane. After evaporation of the solvent, the product could be obtained as a colorless solid (582 mg, 1.6 mmol, 89%). Single crystals suitable for X-ray diffraction analyses were grown by slow vapor diffusion of

https://doi.org/10.1021/acs.organomet.3c00530
Organometallics 2024, 43, 585−593

cyclohexane into a saturated solution of the compound in THF at room temperature. Single crystals of **4a-N**[K@cryptand] suitable for X-ray diffraction analyses were grown by slow vapor diffusion of hexane into a saturated solution of the **4a-N** and 1 eq of 2.2.2-cryptand in THF at −30 °C. $^{31}P\{^{1}H\}$-NMR (162 MHz, THF-d_8): δ = −6.92 (s, PPh_2N) ppm. ^{1}H NMR (400 MHz, THF-d_8): δ = 8.05−7.89 (m, 4H, $NPPh_2H_{Ph,ortho}$), 7.33−7.15 (m, 6H, $NPPh_2H_{Ph,meta}$), 6.63 (br, s, 4H, *p*-tolyl$H_{Ph,ortho,meta}$), 2.08 (s, 3H, *p*-tolylCH_3) ppm. $^{13}C\{^{1}H\}$-NMR (101 MHz, THF-d_8): δ = 153.15 (d, $^{1}J_{CP}$ = 3.40 Hz *p*-tolyl$CH_{Ph,ipso}$), 141.07 (d, $^{2}J_{CP}$ = 41.3 Hz, PCCO), 140.66 (d, $^{1}J_{CP}$ = 113.3 Hz, $NPPh_2CH_{Ph,ipso}$), 132.51 (d, $^{2}J_{CP}$ = 11.5 Hz, $NPPh_2CH_{Ph,ortho}$), 129.85 (d, $^{4}J_{CP}$ = 2.9 Hz, $NPPh_2CH_{Ph,para}$), 129.75 (d, $^{1}J_{CP}$ = 2.3 Hz *p*-tolyl$CH_{Ph,meta}$), 128.21 (d, $^{3}J_{CP}$ = 12.3 Hz, $NPPh_2CH_{Ph,meta}$), 122.55 (s, *p*-tolyl$CH_{Ph,para}$), 122.49 (d, $^{2}J_{CP}$ = 22 Hz *p*-tolyl$CH_{Ph,ortho}$), 20.89 (*p*-tolylCH_3), −1.58 (d, $^{1}J_{CP,PPh2N}$ = 183.7 Hz, PCCO) ppm. Anal. calcd for $C_{21}H_{17}KNOP$: C, 68.27; H, 4.64; N, 3.79. Found: C,68.12; H, 4.66; N, 3.83.

Synthesis of 4a-O. 2.00 g (4.20 mmol) of compound **2a-O** was dissolved in 100 mL of toluene, and 0.56 g (4.23 mmol) of benzyl potassium was added. The reaction was stirred for 20 min at room temperature and the atmosphere in the flask was changed from argon to CO. After 24 h, the reaction was filtered, and the precipitate was washed with toluene and pentane. The solid was dried *in vacuo* to obtain **4a-O** as a colorless solid (1.01 g, 3.60 mmol, 86%). Single crystals of **4a-O**[K@cryptand] suitable for X-ray diffraction analyses were grown by vapor diffusion of hexane in saturated solution of 1 eq **4a-O** and 1 eq of 2.2.2-cryptand in THF. $^{31}P\{^{1}H\}$-NMR (162 MHz, THF-d_8): δ = 13.2 (s, PPh_2O) ppm. ^{1}H NMR (400 MHz, THF-d_8): δ = 7.96−7.59 (m, 4H; $PPh_2OH_{Ph,ortho}$), 7.32−7.07 (m, 6H, $PPh_2OH_{Ph,meta,para}$) ppm. $^{13}C\{^{1}H\}$-NMR (101 MHz, THF-d_8): δ = 143.16 (d, $^{1}J_{CP,PPh2O}$ = 115.8 Hz; $PPh_2OC_{Ph,ipso}$), 140.78 (d, $^{2}J_{CP,PPh2O}$ *J* = 47.5 Hz; PCCO), 131.78 (d, $^{4}J_{CP,PPh2O}$ = 10.5 Hz, $PPh_2OC_{Ph,ortho}$), 130.04 (d, $^{4}J_{CP,PPh2O}$ = 2.7 Hz, $PPh_2OC_{Ph,para}$), 128.45 (d, $^{3}J_{CP,PPh2O}$ = 12.2 Hz; $PPh_2OC_{Ph,meta}$), 3.11 (d, $^{1}J_{CP,PPh2O}$ = 209.6 Hz; PCCO) ppm. Anal. calcd for $C_{14}H_{10}PO_2K$: C, 59.99; H, 3.60. Found: C, 60.40; H, 3.91.

Synthesis of 4b-O. 375 mg (0.768 mmol) of compound **2b-O** was dissolved in 50 mL of toluene, and 102 mg (0.783 mmol) of benzyl potassium was added. The reaction was stirred for 20 min, and the atmosphere in the flask was changed from argon to CO. After 24 h, the reaction was filtered, and the precipitate was washed with toluene and then pentane. The solid was dried *in vacuo* to obtain **4b-O** as a white solid (178 mg, 0.609 mmol, 79%). Single crystals of **4b-O**[K@cryptand] suitable for X-ray diffraction analyses were grown by vapor diffusion of hexane in saturated solution of 1 eq **4b-O** and 1 eq of 2.2.2-cryptand in THF/toluene. $^{31}P\{^{1}H\}$-NMR (162 MHz, DMSO-d_6): δ = 31.53 (s, PCy_2O) ppm. ^{1}H NMR (400 MHz, DMSO-d_6): δ = 1.89−1.57 (m, 10H, PCy_2OH_{Cy}), 1.46−0.94 (m, 12H, PCy_2OH_{Cy}) ppm. $^{13}C\{^{1}H\}$-NMR (101 MHz, DMSO-d_6): δ = 135.57 (d, $^{2}J_{CP,PCy2O}$ = 39.8 Hz, PCCO), 38.17 (d, $^{1}J_{CP,PCy2O}$ = 83.1 Hz, $PCy_2OC_{Cy,ipso}$), 26.42 (d, $^{2}J_{CP,PCy2O}$ = 5.5 Hz, $PCy_2OC_{Cy,ortho}$), 26.29 (d, $^{2}J_{CP,PCy2O}$ = 5.4 Hz, $PCy_2OC_{Cy,ortho}$), 26.28 (d, $^{3}J_{CP,PCy2O}$ = 1.2 Hz, $PCy_2OC_{Cy,meta}$), 26.19 (d, $^{3}J_{CP,PCy2O}$ = 1.2 Hz, PCy2O$C_{Cy,meta}$), 25.35 (s, $PCy_2OC_{Cy,para}$), 25.32 (s, $PCy_2OC_{Cy,para}$), 0.17(d, $^{1}J_{CP,PCy2O}$ = 182.7 Hz, PCCO) ppm. Anal. Calcd for $C_{14}H_{22}PO_2K$: C, 57.51; H, 7.58. Found: C, 57.74; H, 7.28.

Synthesis of 4b-S. 1.00 g (2.12 mmol) of compound **1b** and 0.06 g (2.01 mmol) of elemental sulfur were dissolved together in 30 mL of toluene. After the solution was stirred for 15 min at room temperature, 0.55 g (4.23 mmol) of benzyl potassium were added, and the solution was stirred again for 20 min. After filtration, the atmosphere in the flask was changed from argon to CO, and the reaction was stirred for 24 h. 30 mL of hexane were added, and the solution was filtered. The filtered solid was washed with toluene and pentane. After evaporation of the solvent, the product could be obtained as a colorless solid (464 mg, 1.5 mmol, 71%). Single crystals suitable for X-ray diffraction analyses were grown by slow vapor diffusion of hexane into a saturated solution of the compound in THF. Suitable single crystals of **4b-S**[K@cryptand] for X-ray diffraction analyses were grown by a saturated solution of 4b-S and 1 equiv of 2.2.2-cryptand in THF. $^{31}P\{^{1}H\}$-NMR (162 MHz, THF-d_8): δ = 43.24 (s, PCy_2S). ^{1}H NMR (400 MHz, THF-d_8): δ = 2.02−1.86 (m, 4H, PCy_2SH_{Cy}), 1.82−1.70 (m, 4H, PCy_2SH_{Cy}), 1.68−1.11 (m, 14H, PCy_2SH_{Cy}). $^{13}C\{^{1}H\}$-NMR (101 MHz, THF-d_8): δ = 139.88 (d, $^{2}J_{CP,PCy2S}$ = 35.2 Hz, PCCO), 42.06 (d, $^{1}J_{CP,PCy2S}$ = 63.5 Hz, $PCy_2SC_{Cy,ipso}$), 27.90 (d, $^{2}J_{CP,PCy2S}$ = 7.6 Hz, $PCy_2SC_{Cy,ortho}$), 27.76 (d, $^{2}J_{CP,PCy2S}$ = 8.1 Hz, $PCy_2SC_{Cy,ortho}$), 27.53 (d, $^{3}J_{CP,PCy2S}$ = 1.6 Hz, $PCy_2SC_{Cy,meta}$), 27.29 (s, $PCy_2SC_{Cy,para}$), 27.26 (s, $PCy_2SC_{Cy,para}$), 26.82 (d, $^{3}J_{CP,PCy2S}$ = 1.9 Hz, PCy2S$C_{Cy,meta}$), −2.39 (d, $^{1}J_{CP,PCy2S}$ = 152.2 Hz, PCCO). Anal. calcd for $C_{14}H_{22}PSOK$: C, 54.51; H, 7.19; S, 10.40 Found: C, 54.63; H, 7.33; S, 10.16.

Synthesis of 4a-Se. 300 mg (0.56 mmol) of 2a-Se and 234 mg (1.12 mmol) of KHMDS were dissolved in 10 mL of toluene/THF(9:1) mixture. The solution was stirred for 20 min. After filtration, the atmosphere in the flask was changed from argon to CO and the reaction was stirred for 24 h. The solution was concentrated to 5 mL, and precipitation resulted. The solid was filtered and washed with toluene (3 times) and pentane (3 times). The solid was dried to yield **4a-Se** as off-white solid.(119 mg, 0.38 mmol, 62%). Single crystals of **4a-Se** were grown by slow diffusion of cyclohexene into solution of 1 eq **4a-Se** and 1 eq of 2.2.2-cryptand in THF/toluene. $^{31}P\{^{1}H\}$-NMR (162 MHz, THF-d_8): δ = 6.24 (s, PPh_2Se) ppm. ^{1}H NMR (400 MHz, THF-d_8): δ = 8.12−8.01 (m, 4H, $PPh_2SeH_{Ph,ortho}$), 7.26−7.18 (m, 6H, $PPh_2SeH_{Ph,meta,para}$). $^{13}C\{^{1}H\}$-NMR (101 MHz, THF-d_8): δ = 143.86 (d, $^{2}J_{CP,PPh2Se}$ = 39.0 Hz, PCCO), 143.01 (d, $^{1}J_{CP,PPh2Se}$ = 85.1 Hz, $PPh_2SeC_{Ph,ipso}$), 131.93 (d, $^{2}J_{CP,PPh2Se}$ = 11.9 Hz, $PPh_2SeC_{Ph,ortho}$), 129.76 (d, $^{4}J_{CP,PPh2Se}$ = 3.0 Hz, $PPh_2SeC_{Ph,meta}$), 128.00 (d, $^{3}J_{CP,\ PPh2Se}$ = 12.7 Hz, $PPh_2SeC_{Ph,meta}$), 2.51 (d, $^{1}J_{CP,PPh2Se}$ = 163.8 Hz, PCCO). ^{77}Se-NMR (76 MHz, THF-d_8): δ = 138.10 (d, $^{1}J_{PSe}$ = 650.36 Hz, PPh_2Se) ppm.

■ ASSOCIATED CONTENT

Supporting Information

The Supporting Information is available free of charge on the ACS Publications Web site. The Supporting Information is available free of charge at https://pubs.acs.org/doi/10.1021/acs.organomet.3c00530.

General procedures, NMR and IR spectra of all compounds (PDF)

Details to the DFT calculations and crystal structure analyses (XYZ)

Accession Codes

CCDC 2320765−2320774 contain the supplementary crystallographic data for this paper. These data can be obtained free of charge via www.ccdc.cam.ac.uk/data_request/cif, or by emailing data_request@ccdc.cam.ac.uk, or by contacting The Cambridge Crystallographic Data Centre, 12 Union Road, Cambridge CB2 1EZ, U.K; fax: +44 1223 336033.

■ AUTHOR INFORMATION

Corresponding Author

Viktoria H. Gessner − *Faculty of Chemistry and Biochemistry, Ruhr-University Bochum, 44801 Bochum, Germany;* orcid.org/0000-0001-6557-2366; Email: viktoria.gessner@rub.de

Authors

Mike Jörges − *Faculty of Chemistry and Biochemistry, Ruhr-University Bochum, 44801 Bochum, Germany*

Sunita Mondal − *Faculty of Chemistry and Biochemistry, Ruhr-University Bochum, 44801 Bochum, Germany*

Manoj Kumar − *Faculty of Chemistry and Biochemistry, Ruhr-University Bochum, 44801 Bochum, Germany*

Prakash Duari − *Faculty of Chemistry and Biochemistry, Ruhr-University Bochum, 44801 Bochum, Germany*

Felix Krischer − *Faculty of Chemistry and Biochemistry, Ruhr-University Bochum, 44801 Bochum, Germany*

Julian Löffler − *Faculty of Chemistry and Biochemistry, Ruhr-University Bochum, 44801 Bochum, Germany*

Complete contact information is available at: https://pubs.acs.org/10.1021/acs.organomet.3c00530

Author Contributions

†S.M., M.K. and P.D. contributed equally to this work.

Notes

The authors declare no competing financial interest.

■ ACKNOWLEDGMENTS

Funded by the Deutsche Forschungsgemeinschaft (DFG, German Research Foundation) under Germany's Excellence Strategy—EXC-2033−390677874—RESOLV, and INST 213/917-1 FUGG as well as the European Union (ERC, CarbFunction, 101086951). Views and opinions expressed are however those of the author(s) only and do not necessarily reflect those of the European Union or the European Research Council. Neither the European Union nor the granting authority can be held responsible for them.

■ REFERENCES

(1) Staudinger, H. Ketene, eine neue Körperklasse. *Chem. Ber.* **1905**, *38*, 1735−1739.
(2) Allen, A. D.; Tidwell, T. T. Recent advances in ketene chemistry. *Arkivoc* **2017**, *2016* (1), 415−490.
(3) Allen, A. D.; Tidwell, T. T. Ketenes and other cumulenes as reactive intermediates. *Chem. Rev.* **2013**, *113* (9), 7287−7342.
(4) *Science of Synthesis: Houben-Weyl Methods of Molecular Transformations, Paper Archive Copy, 23 = Category 3*; Aizpurua, J. M.; Danheiser, R. L.; Bellus, D.; Houben, J.; Weyl, T., Eds.; Thieme, 2006.
(5) Radhoff, N.; Studer, A. 1,4-Aryl migration in ketene-derived enolates by a polar-radical-crossover cascade. *Nat. Commun.* **2022**, *13* (1), No. 3083, DOI: 10.1038/s41467-022-30817-3.
(6) Allen, A. D.; Tidwell, T. T. Chapter Four - Structure and Mechanism in Ketene *Chemistry. In Advances in Physical Organic Chemistry*; Williams, I. H.; Williams, N. H., Eds.; Academic Press 2014; pp 229−324.
(7) Shindo, M. Ynolates as Functional Carbanions. *Synthesis* **2003**, *15*, 2275−2288.
(8) Schöllkopf, U.; Hoppe, I. Lithium Phenylethynolate and Its Reaction with Carbonyl Compounds to Give β-Lactones. *Angew. Chem., Int. Ed.* **1975**, *14* (11), 756 DOI: 10.1002/anie.197507651.
(9) Zhang, Z.; Zhang, Y.; Wang, J. Carbonylation of Metal Carbene with Carbon Monoxide: Generation of Ketene. *ACS Catal.* **2011**, *1* (11), 1621−1630.
(10) Woodbury, R. P.; Long, N. R.; Rathke, M. W. Reaction of Trimethylsilylketene with Strong Base. Evidence for Ketene Enolate Formation. *J. Org. Chem.* **1978**, *43* (2), 376.
(11) Kai, H.; Iwamoto, K.; Chatani, N.; Murai, S. Ynolates from the Reaction of Lithiosilyldiazomethane with Carbon Monoxide. New Ketenylation Reactions. *J. Am. Chem. Soc.* **1996**, *118* (32), 7634−7635.
(12) Hillhouse, G. L. Metalloketene formation by insertion of carbon suboxide into tungsten and rhenium metal-hydride bonds. *J. Am. Chem. Soc.* **1985**, *107* (25), 7772−7773.
(13) List, A. K.; Hillhouse, G. L.; Rheingold, A. L. A carbon-carbon bond cleavage reaction of carbon suboxide at a metal center. Synthesis and structural characterization of $WCl_2(CO)(PMePh_2)_2$\{C,C':.eta.2-C(O)CPMePh$_2$\}. *J. Am. Chem. Soc.* **1988**, *110* (14), 4855−4856.
(14) (a) Paiaro, G.; Pandolfo, L.; Morandini, F.; Fioretto, S. D. Stereochemical pattern of phosphine oxidation by a peroxometallacyclic platinum complex. Evidence of an intramolecular process. *J. Organomet. Chem.* **1994**, *483*, 147−151. (b) Pandolfo, L.; Paiaro, G.; Ganis, P.; Valle, G.; Traldi, P. Reactivity of a platinum η1-formylketenyl complex synthesis of a platinum α-pyrone derivative via generation and trapping of a C3H2O2 species. 20. *Inorg. Chim. Acta* **1993**, *210* (1), 39−45.
(15) Kowalski, C. J.; Fields, K. W. Alkynolate anions via a new rearrangement: the carbon analog of the Hofmann reaction. *J. Am. Chem. Soc.* **1982**, *104* (1), 321−323.
(16) Satoh, T.; Nakamura, A.; Iriuchijima, A.; Hayashi, Y.; Kubota, K. A new synthesis of β,γ-alkenyl carboxylic acids from α,β-alkenyl carboxylic acid chlorides and α,β-alkenyl aldehydes with one-carbon elongation. *Tetrahedron* **2001**, *57* (48), 9689−9696.
(17) Ito, M.; Shirakawa, E.; Takaya, H. Generation of Silylethynolates via C-Si Bond Cleavage of Disilylketenes Induced by t -BuOK. *Synlett* **2002**, *2002* (8), 1329−1331.
(18) Hoppe, I.; Schöllkopf, U. Über Lithiumalkinolate und lithiierte Ketene. *Liebigs Ann. Chem.* **1979**, *1979* (2), 219−226.
(19) Kowalski, C. J.; Lal, G. S. Lithium hydride addition to ynolate anions: the mechanism of reductive ester homologation. *J. Am. Chem. Soc.* **1986**, *108* (17), 5356−5357.
(20) Xu, M.; Wang, T.; Qu, Z.-W.; Grimme, S.; Stephan, D. W. Reactions of a Dilithiomethane with CO and N_2O: An Avenue to an Anionic Ketene and a Hexafunctionalized Benzene. *Angew. Chem., Int. Ed.* **2021**, *60* (48), 25281−25285.
(21) Jörges, M.; Krischer, F.; Gessner, V. H. Transition metal-free ketene formation from carbon monoxide through isolable ketenyl anions. *Science* **2022**, *378* (6626), 1331−1336.
(22) For ligand exchange reactions in neutral carbon bases, see: (a) Antoni, P. W.; Reitz, J.; Hansmann, M. M. N_2/CO Exchange at a Vinylidene Carbon Center: Stable Alkylidene Ketenes and Alkylidene Thioketenes from 1,2,3-Triazole Derived Diazoalkenes. *J. Am. Chem. Soc.* **2021**, *143*, 12878−12885. (b) Antoni, P. W.; Golz, C.; Holstein, J. J.; Pantazis, D. A.; Hansmann, M. M. Isolation and reactivity of an elusive diazoalkane. *Nat. Chem.* **2021**, *13*, 587−593. (c) Feuerstein, W.; Varava, P.; Fadaei-Tirani, F.; Scopelliti, R.; Severin, K. Synthesis, structural characterization, and coordination chemistry of imidazole-based alkylidene ketenes. *Chem. Commun.* **2021**, *57*, 11509−11512. (d) Hansmann, M. M. Transition Metal-Free Activation of Carbon Monoxide: Ketenyl Anions by PPh_3/CO Exchange. *Angew. Chem., Int. Ed.* **2023**, *62*, No. e202301826, DOI: 10.1002/anie.202301826. (e) Alcarazo, M.; Lehmann, C. W.; Anoop, A.; Thiel, W.; Fürstner, A. Coordination Chemistry at Carbon. *Nat. Chem.* **2009**, *1*, 295−301.
(23) Krischer, F.; Jörges, M.; Leung, T.-F.; Darmandeh, H.; Gessner, V. H. Selectivity Control of the Ligand Exchange at Carbon in α-Metallated Ylides as Route to Ketenyl Anions. *Angew. Chem., Int. Ed.* **2023**, *62*, No. e202309629, DOI: 10.1002/anie.202309629.
(24) Wei, R.; Wang, X.-F.; Ruiz, D. A.; Liu, L. L. Stable Ketenyl Anions via Ligand Exchange at an Anionic Carbon as Powerful Synthons. *Angew. Chem., Int. Ed.* **2023**, *62* (15), No. e202219211, DOI: 10.1002/anie.202219211.
(25) Jörges, M.; Kroll, A.; Kelling, L.; Gauld, R.; Mallick, B.; Huber, S. M.; Gessner, V. H. Synthesis, Crystal and Electronic Structures of a Thiophosphinoyl- and Amino-Substituted Metallated Ylide. *ChemistryOpen* **2021**, *10* (11), 1089−1094.
(26) Scherpf, T.; Wirth, R.; Molitor, S.; Feichtner, K.-S.; Gessner, V. H. Bridging the Gap between Bisylides and Methandiides: Isolation, Reactivity, and Electronic Structure of an Yldiide. *Angew. Chem., Int. Ed.* **2015**, *54* (29), 8542−8546.
(27) Schwarz, C.; Scharf, L. T.; Scherpf, T.; Weismann, J.; Gessner, V. H. Isolation of the Metalated Ylides Ph3P-C-CNM (M = Li, Na, K): Influence of the Metal Ion on the Structure and Bonding Situation. *Chem. - Eur. J.* **2019**, *25* (11), 2793−2802, DOI: 10.1002/chem.201805421.
(28) Darmandeh, H.; Scherpf, T.; Feichtner, K.-S.; Schwarz, C.; Gessner, V. H. Synthesis, Isolation and Crystal Structures of the Metalated Ylides Cy3P-C-SO2TolM (M = Li, Na, K). *Z. Allg. Anorg. Chem.* **2020**, *646* (13), 835−841.
(29) Baumgartner, T.; Schinkels, B.; Gudat, D.; Nieger, M.; Niecke, E. Lithium Phosphoranylidene Ylides Mes*-P(E)C(H)Li(THF) 3 (E = NMes*, C(SiMe 3) 2): Synthesis, Crystal Structure, and Transmetalation. *J. Am. Chem. Soc.* **1997**, *119* (50), 12410−12411.

(30) Goumri-Magnet, S.; Gornitzka, H.; Baceiredo, A.; Bertrand, G. Synthetic Utility of Stable Phosphanylcarbenes: Synthesis and Crystal Structure of anα-(Lithiomethylene)phosphorane. *Angew. Chem., Int. Ed.* **1999**, *38* (5), 678−680.
(31) Bent, H. A. An Appraisal of Valence-bond Structures and Hybridization in Compounds of the First-row elements. *Chem. Rev.* **1961**, *61* (3), 275−311.
(32) McAllister, M. A.; Tidwell, T. T. Structural and substituent effects on the ketene infrared stretching frequency. *Can. J. Chem.* **1994**, *72* (3), 882−887.
(33) Perdew, J. P.; Burke, K.; Ernzerhof, M. Generalized Gradient Approximation Made Simple. *Phys. Rev. Lett.* **1996**, *77* (18), 3865−3868.
(34) Knizia, G. Intrinsic Atomic Orbitals: An Unbiased Bridge between Quantum Theory and Chemical Concepts. *J. Chem. Theory Comput.* **2013**, *9* (11), 4834−4843.
(35) Bailey, P. J.; Coxall, R. A.; Dick, C. M.; Fabre, S.; Henderson, L. C.; Herber, C.; Liddle, S. T.; Loroño-González, D.; Parkin, A.; Parsons, S. The first structural characterisation of a group 2 metal alkylperoxide complex: comments on the cleavage of dioxygen by magnesium alkyl complexes. *Chem. - Eur. J.* **2003**, *9* (19), 4820−4828, DOI: 10.1002/chem.200305053.
(36) Intrinsic bond orbitals are localized molecular orbitals. IBO1 and IBO2 are the localized versions of the HOMO and HOMO-1. For further details, see ref 34 and Knizia, G.; Klein, J. Electron flow in reaction mechanisms—revealed from first principles. *Angew. Chem., Int. Ed.* **2015**, *54*, 5518.

https://doi.org/10.1021/acs.organomet.3c00530
Organometallics 2024, 43, 585−593